Turbulent Diffusion of Heat at High Rayleigh Numbers

Joseph J. Niemela

Abstract Thermal convection is observed in controlled laboratory experiments at very high Rayleigh numbers using a relatively large apparatus filled with low temperature helium gas. The low temperature environment offers two advantages toward the study of turbulent convection; namely the favorable properties of the working fluid in achieving very high Rayleigh numbers and the low thermal mass of the heated metallic surfaces at cryogenic temperatures. The latter property is exploited in order to provide a means of measuring an effective thermal diffusion coefficient of the buoyancy-driven turbulence by propagating thermal waves into the bulk and observing the damping of their amplitude with distance. The diffusivity measured directly in this way compares well with values inferred from the time-independent measurements of the global turbulent heat transfer at Rayleigh numbers of order 10^9 but are significantly different at Rayleigh numbers of order 10^{13} which can be interpreted as a consequence of the formation of well developed bulk turbulence decoupled from the thermal boundary layers at the heated horizontal surfaces.

1 Introduction

Thermal convection is common to many natural and engineering systems, and turbulence in these flows is more the rule than the exception, especially for large scale natural phenomena. Familiar examples are convection in stars, in the outer core of the earth, and in the atmosphere. Considering stellar convection alone, we could argue that turbulent convection itself is the most ubiquitous type of flow that we know of. Unfortunately, the values of the principal control parameter for stellar convection are quite high and pose problems for laboratory experiments, notwithstanding the

J. J. Niemela (✉)
The Abdus Salam International Centre for Theoretical Physics, ICTP, Strada Costiera 11, 34014 Trieste, Italy
e-mail: niemela@ictp.it

L. Di G. Sigalotti et al. (eds.), *Computational and Experimental Fluid Mechanics with Applications to Physics, Engineering and the Environment*, Environmental Science and Engineering,
DOI:10.1007/978-3-319-00191-3_2, © Springer International Publishing Switzerland 2014

obvious difficulties in matching fluid properties and boundary conditions. If we concentrate on the first problem, namely the principal control parameter, and simplify the rest of the problem by selecting an artificial system with well defined boundary conditions, we have the possibility to make some progress. This assumes, of course, that in doing this we retain the essential physics of the problem. It is important to note that even a relatively simple system becomes highly nonlinear at high values of the control parameter, and therefore poses a challenging problem in itself. The system referred to here is Rayleigh-Bénard convection (RBC), in which a layer of fluid is contained between two heated horizontal surfaces. The upper (lower) surface is cooled (heated) so that a mechanically unstable density gradient is formed across the fluid layer, which is assumed to be thin, in the sense that we can neglect compressibility effects. In actuality, compressibility cannot be entirely neglected, and a correction for adiabatic temperature gradients is necessary. We also confine our attention to fluids for which the coefficient of thermal expansion has a reversed sign, requiring the opposite heating arrangement (e.g. water below 4 °C). Any parcel of, say, hot fluid near the lower boundary is subject to buoyancy forces which promote its vertical rise, leading to convective currents, with the same consideration applying to cold fluid near the top of the layer. The degree to which buoyancy overcomes dissipative processes and can lead to convection is given by the dimensionless Rayleigh number Ra given by

$$\mathrm{Ra} = \frac{g\alpha \Delta T H^3}{\nu\kappa}, \tag{1}$$

where α, ν and κ are, respectively, the isobaric thermal expansion coefficient, kinematic viscosity and thermal diffusivity of the fluid, ΔT the temperature difference across the fluid layer of height H and g the acceleration due to gravity. The interplay between heat and momentum diffusion is important, especially for turbulent convection, and that is characterized by the Prandtl number

$$\mathrm{Pr} = \frac{\nu}{\kappa}. \tag{2}$$

2 Apparatus

The apparatus and methodology for the present work has been described in detail in Niemela and Sreenivasan (2003, 2006, 2008). In brief, the fluid—in this case helium gas near 5 K—is held between two OHFC copper plates separated vertically by thin cylindrical stainless steel sidewalls with a fixed diameter of 50 cm. The height of the fluid layer in these experiments was either 50 or 12.5 cm, so that the diameter-to-height aspect ratio was $\Gamma = 1$ or 4, respectively. The OHFC copper used for the heated horizontal surfaces was annealed to have a conductivity near 1 kW $\mathrm{m}^{-1}\mathrm{K}^{-1}$ at helium temperatures. More importantly, it is nearly five orders

of magnitude larger than the molecular conductivity of the working fluid so that the corresponding Biot number is extremely small. This means that constant temperature conditions are assured even when the fluid is turbulent. Heating is provided by a serpentine metallic film encased in mylar and sandwiched to the top and bottom plates by additional copper plates. The top plate is regulated to have constant temperature and is connected through a variable resistance to liquid helium bath which acts as the cold reservoir. Outside the sample space a common cryo-pumped vacuum provides protection against either conductive or convective heating in parallel, and radiative heating is controlled through the use of various concentric shields surrounding the sample space, the inner-most one being at the temperature of the top plate.

Mean pressure is measured by a Baratron gauge, using heads appropriate to the absolute pressure so as to maximize resolution. Temperature measurements rely on semiconductor resistance thermometers made of doped germanium. Within the fluid, cubes of neutron transmutation doped germanium, 250 μ on a side, are used to monitor temperature fluctuations.

The fluid has some special properties: its kinematic viscosity ν can be quite small when the density is large (i.e, near the critical point). The thermal expansion coefficient α is naturally large in the ideal gas limit, as its value is simply the inverse of the absolute temperature. The thermal diffusivity can be both very small and very large depending on the operating point in the pressure-temperature phase space. That is, near the critical point (at 5.2 K) the specific heat C_P diverges and so the thermal diffusivity $\kappa = k/\rho C_P$ vanishes, where k and ρ are, respectively, the thermal conductivity of the fluid and its density. In addition, α is thermodynamically related to the specific heat and so it also gets quite large near the critical point. Taken together, cryogenic helium gas presents a widely tunable fluid that allows both extremely large values of the principal control parameter Ra but also large ranges of it.

3 An Effective Diffusivity

Let us consider the simple diffusion equation

$$\frac{\partial T}{\partial t} = \kappa \frac{\partial^2 T}{\partial x_j \partial x_j}. \tag{3}$$

Under conditions of fully developed bulk turbulence (i.e. decoupled from any solid boundaries) we may consider that the turbulence can be modeled as a "fluid" having an effective diffusivity κ^{eff}. We may then consider Eq. (3), with an effective diffusivity κ^{eff} replacing the molecular value κ. The corresponding time scale, then, for turbulent diffusion is dimensionally given by L^2/κ^{eff} on some characteristic length scale L. On the other hand, we know for turbulent flows with characteristic length scales L and velocity scales u, the corresponding time scale is of order L/u.

Equating the two times scales gives $\kappa^{\text{eff}} \sim uL$. Taking its ratio with the molecular value then gives

$$\frac{\kappa^{\text{eff}}}{\kappa} \sim \frac{uL}{\kappa} = \text{Pe}, \tag{4}$$

where Pe is the Péclet number. From Niemela et al. (2001) we know that $\text{Pe} = 0.13\text{Ra}^{0.50}$. We will return to consider this further below.

For a flow with mean velocity **U** sweeping along a heated surface we may also define an effective heat diffusivity starting with the diffusion-advection equation

$$\frac{\partial T}{\partial t} + U_j \frac{\partial T}{\partial x_j} = \kappa \frac{\partial^2 T}{\partial x_j \partial x_j}. \tag{5}$$

Decomposing velocity and temperature for turbulent flows into mean and fluctuating parts and averaging over the fluctuations (see Tennekes and Lumley 1997) we obtain for the heat transfer

$$q_j = \rho c_P \left(\overline{\theta u_j} - \kappa \frac{\partial T}{\partial x_j} \right), \tag{6}$$

where θ and u represent fluctuating components of temperature and velocity, respectively. By Reynolds' analogy we can define an eddy diffusivity for heat, κ_T as

$$\overline{\theta u_j} = -\kappa_T \frac{\partial T}{\partial x_j} \tag{7}$$

so that we may write for the total heat transfer Q in the vertical direction (for instance)

$$\frac{Q}{\rho c_p} = -(\kappa_T + \kappa) \frac{\partial T}{\partial x_3}. \tag{8}$$

Approximating the gradient in temperature as the average over the entire fluid layer, $H/\Delta T$, and taking as a definition of the dimensionless heat transport the Nusselt number Nu, where Nu is given by

$$\text{Nu} = \frac{QH}{k\Delta T}, \tag{9}$$

we obtain from Eq. (8)

$$\text{Nu} = \frac{\kappa^{\text{eff}}}{\kappa}, \tag{10}$$

where

$$\kappa^{\text{eff}} = \kappa_T + \kappa. \tag{11}$$

It is interesting to note that Eq. (10) can be reconciled with Eq. (4) only if

$$\text{Nu} \sim \text{Ra}^{1/2}. \tag{12}$$

In fact, Eq. (4) resulted from our consideration of a hypothetical fully developed turbulence—i.e., without considering any boundary effects. We know that in the case that the diffusive boundary layers are artificially removed in RBC simulations (Lohse and Toschi 2003), Nu is indeed described by Eq. (12).

4 Time-Dependent Measurements of the Effective Diffusivity

Despite its academic interest, could we in fact measure an effective thermal diffusivity of convective turbulence directly? The thermal diffusivity of solids, or any purely conducting material, can be measured by applying a time-varying temperature at one surface and measuring the damped amplitude or phase of the resulting heat wave at some known distance along the direction of its propagation. The corresponding experiment then is to oscillate the temperature of the bottom boundary of a Rayleigh-Bénard cell and to then measure temperature at that frequency carefully at a known height within the layer. Certainly this will work when the fluid is quiescent, but the question is whether it will work when there are in addition turbulent eddies transporting heat.

The experiment performed was just this: at the top plate we retained a constant temperature as usual, while the bottom plate was subject to a sinusoidally oscillating heat flux with a non-zero mean value giving rise to an oscillation of the bottom plate temperature at the same frequency about some mean value larger than that of the top plate.

Let us consider only the oscillating part of the bottom plate temperature, which is of the form

$$T = T_0 \cos(\omega t). \tag{13}$$

A solution of Eq. (3) satisfying this boundary condition is

$$T = T_0 \exp\left(-\frac{z}{\delta_S}\right) \cos\left(\omega t - \frac{z}{\delta_S}\right), \tag{14}$$

where $\delta_S = (2\kappa/\omega)^{1/2}$ is the penetration depth. Equation (14) describes a wave-like phenomenon whose phase and amplitude depend on the thermal diffusivity of the medium and the frequency ω of the oscillation. Knowing the oscillation frequency, the position of the temperature sensor, and the amplitude of the temperature oscillation

at the plate, the only unknown is the thermal diffusivity, which is then measured. With κ^{eff} in place of κ, Eq. (14) describes a heat wave that experiences damping and phase variation according to an effective penetration depth

$$\delta_{\text{eff}} = \sqrt{\frac{2\kappa^{\text{eff}}}{\omega}}. \tag{15}$$

If we also measure the dimensionless heat transfer or Nusselt number Nu simultaneously, we have two independent measurements of diffusivity: one through Nu, that requires no assumptions but only indirectly gives the diffusivity, and the other which is directly sensitive to the diffusivity but requires that we postulate a turbulent "fluid". To see how Nu infers the diffusivity, we refer to Eq. (9). Multiplying both numerator and denominator by the heat capacity of the fluid we obtain Eq. (10), where we identify $QH/\Delta T$ as the effective thermal conductivity of the fluid and κ^{eff} is then that value multiplied by the heat capacity.

The experiment is aided by the fact that metals at low temperature have high conductivity compared to the fluid, as was noted above, and also have nearly negligible heat capacity compared to the fluid. The resulting low thermal mass allows us to produce large amplitude, high frequency heat waves that can penetrate with detectable amplitude through the entire bulk region.

The frequency of the modulation, f_M (in Hz), was chosen to be both below and above the characteristic frequency of the largest scale circulation. The amplitude was also varied and a dimensionless form is given by

$$\Delta_M = (T_0)_{\text{rms}}/\langle \Delta T \rangle. \tag{16}$$

Here and elsewhere $\langle ... \rangle$ refers to averaging over integral periods of the modulation.

The experimental procedure consisted of applying sinusoidal heating at the bottom with a DC offset and then waiting for at least 200 cycle times of the large scale circulation to reach a statistical steady state before taking measurements. To obtain Nu conventionally, the temperature difference was averaged over integer numbers of the modulation cycle. From this both $<$ Ra $>$ and $<$ Nu $>$ could be computed.

Fluctuations in the temperature within the bulk were measured at the mid-height of the cell, and about 4.4 cm radially inward from the sidewall. This point was 25 cm above the bottom plate for $\Gamma = 1$ and 6.25 cm above the bottom plate for $\Gamma = 4$. Data were collected at a rate of 50 Hz using the off-balance signal from an audio frequency bridge circuit with lock-in detection. By Fourier analysis it was possible to measure the amplitude of the signal due specifically to the heat wave having frequency f_M.

Table 1 Experimental conditions and measurements

Γ	$< \mathrm{Ra} >$	f_M (Hz)	Δ_M	κ (cm^2 s^{-1})	κ^{eff} (cm^2 s^{-1})	$\frac{\kappa}{\kappa^{\mathrm{eff}}}$	$< \mathrm{Nu} >$
1	3.4×10^9	0.01	0.05	4.03×10^{-2}	3.893	96.6	98.6
4	1.9×10^9	0.032	0.15	7.04×10^{-3}	0.583	82.9	81.6
1	4.5×10^{12}	0.04	0.28	7.93×10^{-4}	3.6099	4,535	975.6
1	1.0×10^{13}	0.025	0.22	4.79×10^{-4}	3.31	6,904	1,277

5 Results and Discussion

Table 1 shows experimental conditions and measurements made in both $\Gamma = 1$ and $\Gamma = 4$ cells. In particular, the last two columns show the ratio of measured diffusivities and the measured (time-averaged) Nusselt number. For the first two rows at low Ra, the values in the last two columns are in excellent agreement. This is remarkable given that in two very different-height systems Eq. (14) returns the same effective diffusivity that one would have inferred from the Nu-measurements. However, the situation changes for the last two rows, which correspond to the same $\Gamma = 1$ cell but at much higher Ra. In this case, the measured diffusivity is larger than we would have expected and its ratio with the molecular value is roughly five times that of the measured Nu.

The result is illustrated graphically in Fig. 1. Here we plot the various values of Nu corresponding to the last two columns of Table 1 for $\Gamma = 1$. In addition, values of Nu taken in the absence of modulation, namely those from Niemela and Sreenivasan (2003), are included. The dashed line represents $\mathrm{Ra}^{1/2}$. One striking fact is that $< \mathrm{Nu} >$ and Nu are the same within experimental uncertainty for all Ra, even when the amplitude of modulation is of the same order as the average temperature difference.

The dashed line in Fig. 1 is meant to denote the expected slope of Nu_κ if the effective diffusivity were determined by Eq. (3). It is arbitrarily adjusted to connect through the two upper data points. It is tempting to think that at high Ra we are measuring for the most part pure bulk turbulence by the propagation of heat waves while at lower Ra we are sensitive to extended boundary layers above the heated plates.

The heat transfer measured by Nu or $< \mathrm{Nu} >$ does not require any assumptions about the fluid layer. It is simply the integration of the contributions of all features of the flow, even if the entire contribution is only from two thin boundary layers near the top and bottom plates at high Ra. On the other hand, the heat wave, at a first approximation, is assumed to propagate through a homogeneous medium. The fact that the thermal boundary layer is much smaller than wither the molecular or effective penetration depth (a fact that is true for all Ra investigated here) would seem to validate its use in RBC.

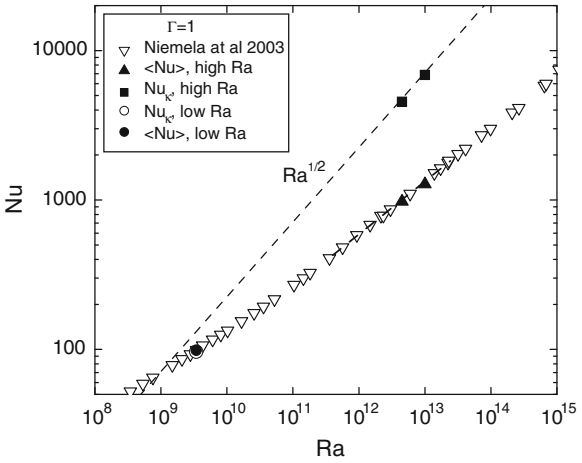

Fig. 1 Nu vs. Ra for $\Gamma = 1$ both with and without modulation. Included are values for Nu_κ as computed by the ratio of the effective to molecular diffusivity. Inverted open triangles, raw Nu from Niemela and Sreenivasan (2003) without modulation; open circles, Nu_κ for low Ra; solid squares, Nu_κ for high Ra; solid circles, $< \mathrm{Nu} >$ for low Ra; solid triangles, $< \mathrm{Nu} >$ for high Ra

It should be noted that Nu can be determined as the ratio between the half-height of the layer and the thermal boundary layer thickness. That is:

$$\mathrm{Nu} \simeq \frac{H}{2\delta}, \tag{17}$$

where δ is the thermal boundary layer thickness. On the other hand, Nu_κ is not dependent on the thermal boundary layer thickness at all, but rather on the ratio between δ_{eff} and δ_S, the effective and molecular Stokes layer thicknesses, respectively, so that

$$\mathrm{Nu}_\kappa \simeq \left(\frac{\delta_{\mathrm{eff}}}{\delta_S}\right)^2. \tag{18}$$

In Niemela and Sreenivasan (2008) it was proposed that the heat wave method "failed" at high Ra due to the emergence of a highly turbulent core region, which was assumed, for simplicity, to have an infinite conductivity. In this situation the amplitude of the heat wave would clearly cease to decrease with distance within the core region, and therefore the position of the sensor would no longer be a relevant parameter (i.e., it could be changed within the core region without affecting the measurement). Note that the conclusions are not really that different than the discussion above; namely, that at very high Ra there may exist a region of well-developed bulk turbulence completely decoupled from the boundaries.

Finally, the data here are few and additional conclusions would clearly benefit from distributed temperature measurements instead of one fixed sensor position and, of course, a larger coverage of Ra. Such experiments are currently underway.

Acknowledgments The author wishes to acknowledge the contribution of K.R. Sreenivasan to the work presented here and the Elettra Synchrotron Facility in Trieste for providing space and support for the experiment.

References

Lohse D, Toschi F (2003) Ultimate state of thermal convection. Phys Rev Lett 90:034502
Niemela JJ, Sreenivasan KR (2003) Confined turbulent convection. J Fluid Mech 481:355–384
Niemela JJ, Skrbek L, Sreenivasan KR, Donnelly RJ (2001) The wind in confined thermal convection. J Fluid Mech 449:169–178
Niemela JJ, Sreenivasan KR (2006) Turbulent convection at high Rayleigh numbers and aspect ratio 4. J Fluid Mech 557:411–422
Niemela JJ, Sreenivasan KR (2008) Formation of the “superconducting” core in turbulent thermal convection. Phys Rev Lett 100:184502
Tennekes H, Lumley JL (1997) A first course in turbulence. The MIT Press, Cambridge

http://www.springer.com/978-3-319-00190-6

Computational and Experimental Fluid Mechanics with Applications to Physics, Engineering and the Environment

Sigalotti, L.D.G.; Klapp, J.; Sira, E. (Eds.)
2014, XXIII, 554 p. 195 illus., 109 illus. in color.,
Hardcover
ISBN: 978-3-319-00190-6